AD-A081 323 DAVID W TAYLOR NAVAL SHIP RESEARCH AND DEVELOPMENT CE--ETC F/G 13/10
A COMPARISON OF COMPUTER PREDICTIONS WITH SCALED MODEL DRAG FOR--ETC(U)
APR 77 C L BERNITT, R O GRAFF, P R SCHEURICH
UNCLASSIFIED DTNSRDC/ASED-TM-16-77-99 NL

END
DATE FILMED
4-80
DDC

DAVID W. TAYLOR NAVAL SHIP RESEARCH AND DEVELOPMENT CENTER

Bethesda, Md. 20084

A COMPARISON OF COMPUTER PREDICTIONS WITH SCALED MODEL DRAG FOR AN AIR CUSHION VEHICLE MODEL AT HIGH CUSHION LOADINGS

by

C. L. Bernitt
R. O. Graff
P. R. Scheurich

AVIATION AND SURFACE EFFECTS DEPARTMENT

April 1977

ASED Technical Memo
16-77-99

MAJOR DTNSRDC ORGANIZATIONAL COMPONENTS

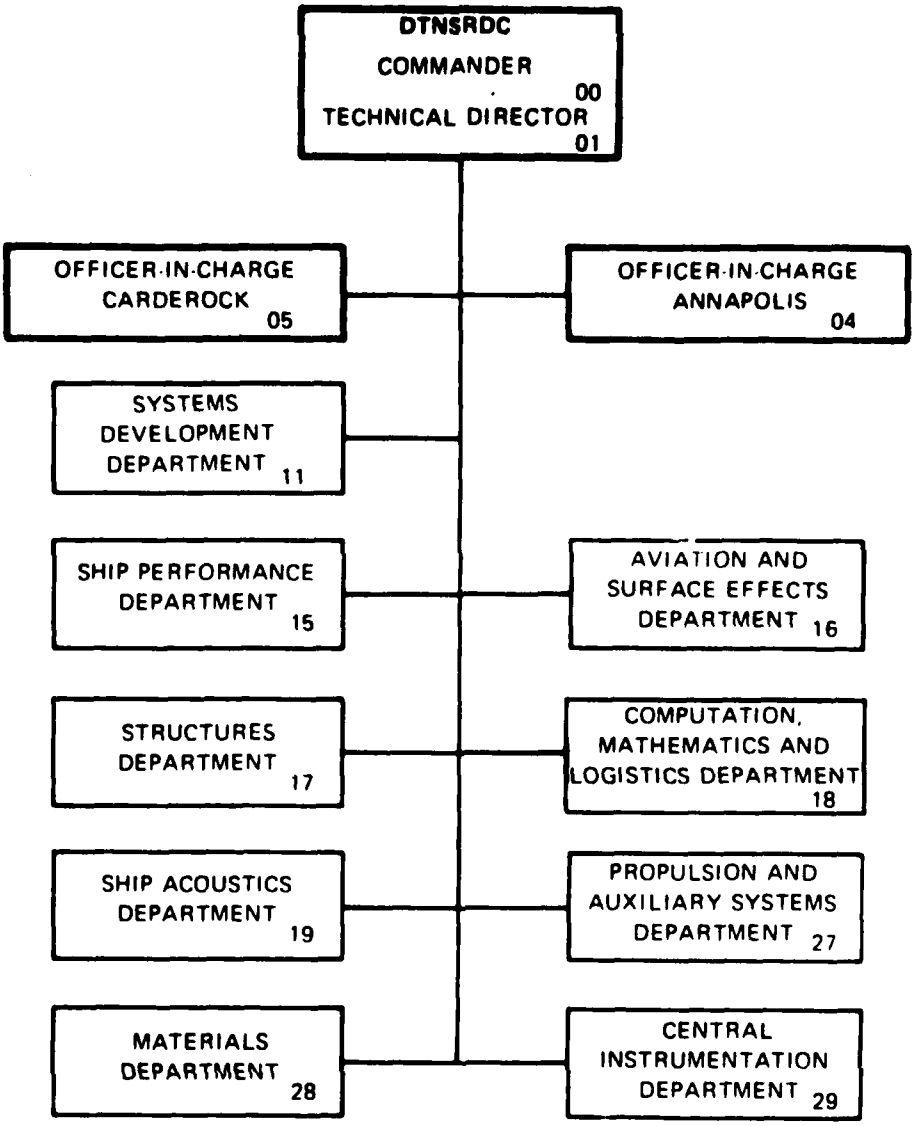

UNCLASSIFIED

SECURITY CLASSIFICATION OF THIS PAGE (When Data Entered)

REPORT DOCUMENTATION PAGE	READ INSTRUCTIONS BEFORE COMPLETING FORM
1. REPORT NUMBER: ASED TM 16-77-99	2. GOVT ACCESSION NO. / 3. RECIPIENT'S CATALOG NUMBER
4. TITLE (and Subtitle): A Comparison of Computer Predictions With Scaled Model Drag For an Air Cushion Vehicle Model at High Cushion Loadings (U)	5. TYPE OF REPORT & PERIOD COVERED / 6. PERFORMING ORG. REPORT NUMBER
7. AUTHOR(s): C. L. Bernitt, R. O. Graff, P. R. Scheurich	8. CONTRACT OR GRANT NUMBER(s)
9. PERFORMING ORGANIZATION NAME AND ADDRESS: DTNSRDC, Bethesda, Maryland 20084	10. PROGRAM ELEMENT, PROJECT, TASK AREA & WORK UNIT NUMBERS
11. CONTROLLING OFFICE NAME AND ADDRESS: CNO (OP96V), Washington, D.C. 20350	12. REPORT DATE: Apr 77 / 13. NUMBER OF PAGES: 35
14. MONITORING AGENCY NAME & ADDRESS (if different from Controlling Office)	15. SECURITY CLASS. (of this report): UNCLASSIFIED / 15a. DECLASSIFICATION/DOWNGRADING SCHEDULE

16. DISTRIBUTION STATEMENT (of this Report)

Unlimited and approved for Public release. Technical memos

17. DISTRIBUTION STATEMENT (of the abstract entered in Block 20, if different from Report)

DTNSRDC/ASED-TM-16-77-99

18. SUPPLEMENTARY NOTES

387 695

19. KEY WORDS (Continue on reverse side if necessary and identify by block number)

Advanced Naval Vehicle Concepts Evaluation
ANVCE
Technology Assessment
Air Cushion Vehicle
Drag
High Cushion Loadings

20. ABSTRACT (Continue on reverse side if necessary and identify by block number)

Using a 3x6 foot model, a series of tests were conducted to investigate the high speed operation, in terms of vehicle performance (DRAG) and ride quality (MOTIONS) of ACV designs with high cushion loading. The scope of this document is limited to an analysis of the drag results only.

3 by 6

DD FORM 1 JAN 73 1473 EDITION OF 1 NOV 65 IS OBSOLETE

UNCLASSIFIED 387695

SECURITY CLASSIFICATION OF THIS PAGE (When Data Entered)

A COMPARISON OF COMPUTER PREDICTIONS WITH SCALED MODEL DRAG FOR AN AIR CUSHION VEHICLE MODEL AT HIGH CUSHION LOADINGS

by

C. L. Bernitt
R. O. Graff
P. R. Scheurich

AVIATION AND SURFACE EFFECTS DEPARTMENT

April 1977

ASED Technical Memo
16-77-99

TABLE OF CONTENTS

LIST OF FIGURES

INTRODUCTION

A series of tow tank experiments utilizing a 0.91 x 1.82 meters (3 x 6 feet) air cushion vehicle (ACV) model were conducted as part of the Advanced Naval Vehicles Concept Evaluation Program (ANVCE). The basic objective of the test series was to investigate the high speed operation, in terms of vehicle performance (drag) and ride quality (motions), of ACV designs with high cushion loading. Very few data are available on ACV's in the range of displacements being investigated in the ANVCE Program. The full scale prototypes to be modeled in this program are in the range of 1,000 - 4,000 metric ton gross weights with cushion loadings, $P_c/\sqrt{S}$, ranging from 100 to 500 N/m^3 (0.64 - 3.18 lb/ft^3). Results from these test series are intended to furnish a high speed data base for ACV's and serve as an input to the ANVCE point design tasks. These results are also to be used to determine the suitability of current drag predictive techniques.

The scope of this document is limited to an analysis of the drag results only. It is intended to compare scaled model drag with that of an ACV performance prediction routine which utilizes currently accepted prediction methods. From these comparisons one can determine if the present prediction program is satisfactorily computing the drag for designs with high cushion loading. The prediction routine is described in Reference 1. A complete description of the test series and the quantities measured is presented in Reference 2.

MODEL DESCRIPTION/TEST CONDITIONS

The model used for this test had a length-to-beam of 2 with a full peripheral, deep skirt design developed for the Advanced Research Projects Agency, Arctic Surface Effect Vehicle Program. The model was built for this test using similar plans to the Aerojet General Corporation's JEFF(A) model for the Amphibious Assault Landing Craft program. The model experiments were conducted in the David W. Taylor Naval Ship Research and Development Center's model basin using the high speed Number II Carriage. The

towing arrangement for the model tests is shown in Figure 1. The model was free to pitch, roll and heave. The hardstructure dimensions of the model are 199.85 cm (78.68 in.) in length, and 16.00 cm (6.3 in.) in width. While the cushion dimensions can change, as will be discussed later, the nominal sizes are a cushion length, ℓ_c, of 182.25 cm (71.75 in), a beam, b_c, of 90.81 cm (35.75 in.), and a cushion depth of 19.20 cm (7.56 in.).

The deep skirt design on the model was configured in the loop-pericell design. Airflow to the skirt was supplied by ten individually controllable Aximax - 3 fans. The fans were arranged with four feeding directly into the cushion and with six feeding into the loop. The fan placement on the model is shown in the diagram below. By turning fans off and by adjusting the rpm, the desired flow rate into the cushion could be selected.

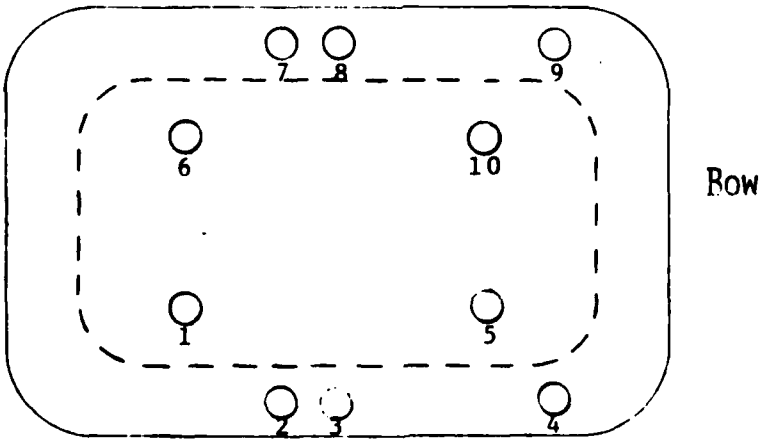

The model was tested at weights of 56.9 kg (125.5 lbs) and 85.4 kg (188.2 lbs) in order to simulate the cushion loadings, $P_c/\sqrt{S}$, of 300 N/m^3 (1.91 lb/ft^3) and 450 N/m^3 (2.86 lb / ft^3) for both the 1,000 and 3,000 m.

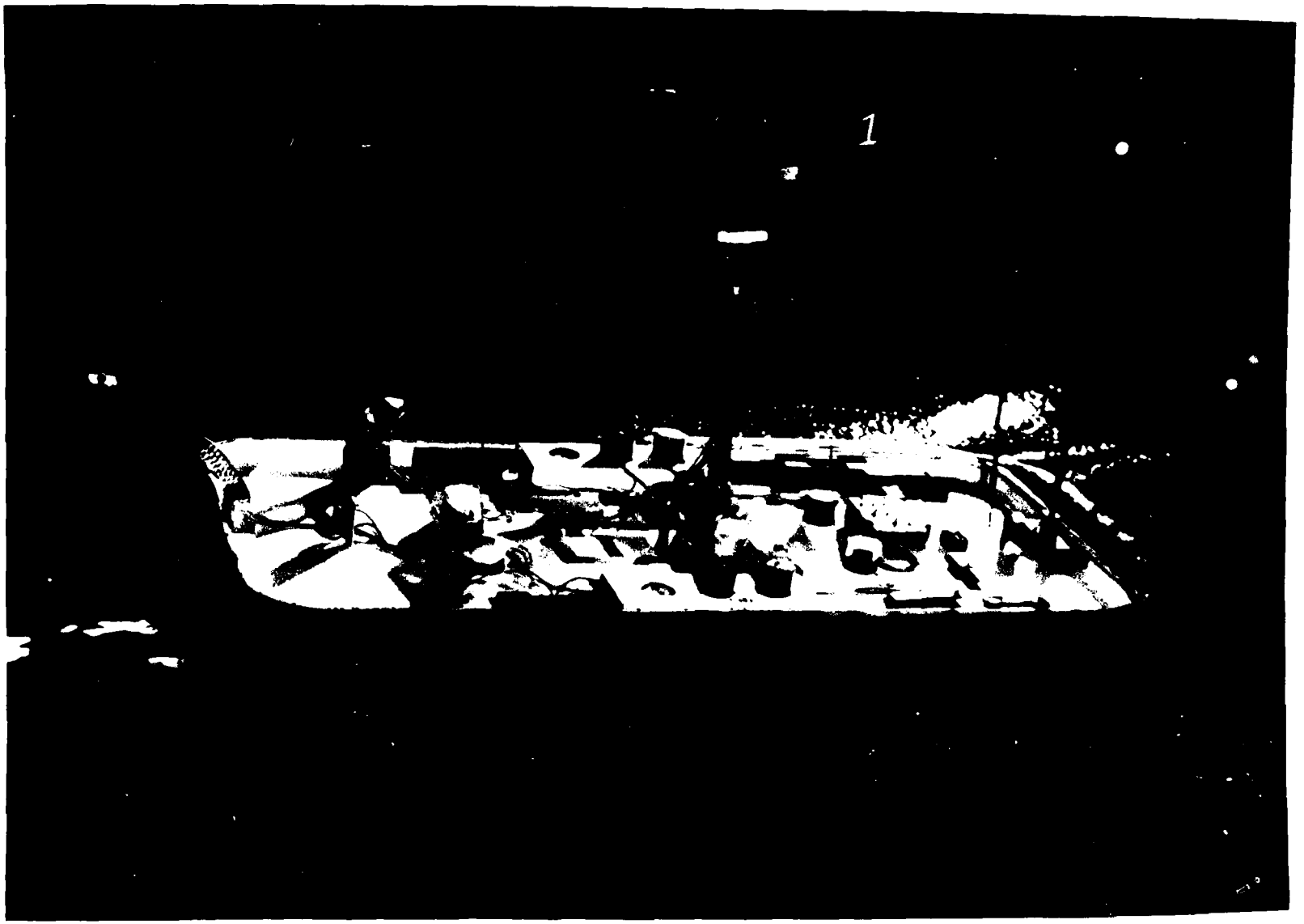

Figure 1 - Experimental Model Operating in Tow Tank

ton full scale designs. Various fan combinations and conditions were selected based upon fan manufacturer pressure/flow rate curves to provide the necessary cushion pressure and volume flow rate. The cushion volume flow rate was varied to simulate model full-scale daylight gap heights, h_g, of .075 - .15 m (.25 - .50 ft.) depending upon the scale factor utilized. The model was tested in both calm water and scaled random waves at various model speeds. The measurements taken at each condition were drag, pitch, heave, vertical c.g., bow and stern accelerations, skirt loop pressures, cushion pressures, structural impact pressures and relative bow motion.

A summary of model cushion characteristics for the two tested configurations is given in Table 1. Also shown are the scale factors, λ, used for Froude scaling the model data to the 1,000 and 3,000 metric ton full scale design. A description of the scaling procedure will be presented later in the report.

In order to determine the necessary model weights for modeling the desired cushion loadings, a nominal value of the cushion area, S, was determined from previous Aerojet General tests of a similar ACV model. After determining the desired cushion pressure, P_c, from the above, the necessary model weight was derived. However, during the experiments, it was found that the pressures were lower than expected which led to the conclusion that the model cushion area was different and apparently changed with model weights. The mean P_c values obtained from the calm water runs are shown in Table 1. The calculated cushion area which increased with model weight is also given in Table 1. The effect of this cushion area variation was to change the expected cushion loading conditions being modeled. The actual nominal cushion loading values were found to be 285 N/m^3 and 400 N/m^3 (1.81 and 2.55 lb/ft^3).

During the test there were several problems with the skirt system. The major problem was with the skirt fabric bonding and attachment. Figure 2 shows the underside of the model where the first problem with the skirts occurred. Skirt material was fastened under the batten, and

TABLE 1

	Case 1	Case 2
Model Weight	85.4 kg (188.2 lb)	56.9 kg (125.5 lb)
Desired $P_c/\sqrt{S}$	450 N/m^3 (2.86 lb/ft^3)	300 N/m^3 (1.91 $lb.ft^3$)
Desired P_c	553.5 N/m^2 (11.56 lb/ft^2)	369.2 N/m^2 (7.71 lb/ft^2)
Actual P_c	510.9 N/m^2 (10.67 lb/ft^2)	356.7 N/m^2 (7.45 lb/ft^2)
Cushion Area (S)	1.64 m^2 (17.64 ft^2)	1.57 m^2 (16.85 ft^2)
Actual $P_c/\sqrt{S}$	400 N/m^3 (2.55 lb/ft^3)	285 N/m^3 (1.81 lb/ft^3)
Scale Factors	$\lambda_{1000} = 22.7$	$\lambda_{1000} = 26.0$
	$\lambda_{3000} = 32.75$	$\lambda_{3000} = 37.5$

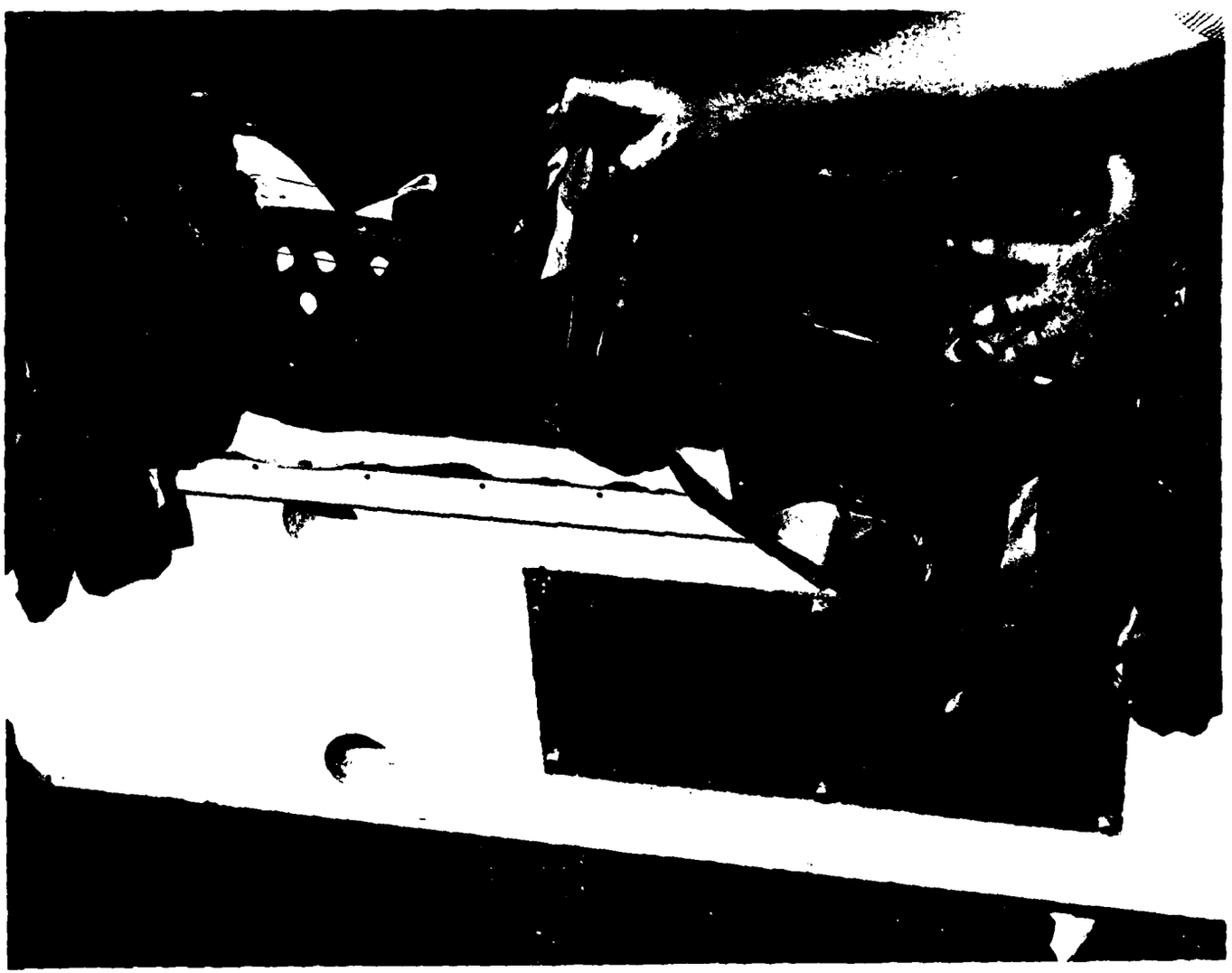

Figure 2 - Underside View of Skirt Glue-Joint Defects

then the cells were glued to this material. This glue joint did not hold up under the test conditions. To correct this problem, all the glue joints were reinforced by sewing the fabric together. This cured the problem for some time, but then the material under the batten pulled loose. This was fixed by moving the batten over slightly and adding more screws into the batten. It is believed that these repairs caused only negligible changes in the skirt geometry.

The repairs described above fixed the construction defects of the model; however, this resulted in substantial delays in testing and eventually necessitated a decrease in the desired number of test conditions that could be investigated. A third cushion loading condition and many more random wave runs would have been desirable. It should also be mentioned that fans 4 and 9 were moved to the forward location from amidship during the repairs in order to improve flow distribution through the loop.

PREDICTION TECHNIQUE

The prediction technique used herein consists of a series of equations which compute the various drag components based on the geometry, gross weight, cushion pressure,and desired gap height of an ACV configuration. The purpose of the technique is to predict the total drag of an ACV design as a function of the design speed, sea state,and wind velocity. The drag equations used in the analysis are presented in Appendix A. The sources for the actual equations are presented in Reference 1 in which the complete parametric design computer program is discussed. The drag computation routine is a part of this program.

The drag equations are based upon basic theory and upon ACV model and full scale experimental data. The expressions for aerodynamic, momentum, and wavemaking drag are accepted state-of-the-art equations that are widely documented. Compared to these equations, the expressions presented in Appendix A for the calm water wetting, skirt related wavemaking and rough water skirt drag represent an attempt by one experienced

contractor to derive parametric equations for predicting these drag components. Each of these empirical equations is based on limited model and full scale experimental data gathered by the contractor. These equations are functions of those design variables that have been shown to significantly affect the magnitude of the skirt drag. Using these component drag equations, the resultant total drags compare favorably with those measured in model experiments. However, due to the tremendous difficulty in isolating these drag components, there is no direct method for verifying the results from any specific equation.

The experiments discussed herein were conducted in part to determine if these equations were applicable for the range of vehicles of interest in the ANVCE Program. The data used to derive the empirical expressions previously discussed are generally limited to state-of-the-art ACV's which weigh up to 200 m. tons and have cushion loadings up to 165 N/m^3. To meet payload and range requirements, ACV's weighing from 1,000 to 4,000 m. tons with cushion loadings up to 500 N/m^3 must be considered. To adequately address the parametric and point design data for these possible conditions, it is necessary to evaluate the applicability of extrapolating the specific empirical expressions to larger gross weight and cushion loadings.

Specific full scale design characteristics were selected which could realistically be achieved within model design constraints and model testing limits. Based on these design characteristics which are presented in Table 2, total drag values were predicted using the equations previously discussed. Inputs to these equations included the full scale gross weight, the cushion loading, the gap height (from model flow rate data) and the wave height characteristics. The over wave or rough water total drag is based on the average wave height and the corresponding sea state wind speed. The sea state conditions used in this analysis are given in Table 3. The predicted total drag values for these conditions will be compared with scaled model test data in a later section.

TABLE 2 - Full Scale Craft Characteristics

	1000 m. tons			3000 m. tons	
$P_c/\sqrt{S}$	285	400	N/m^3	285	400
	(1.81)	(2.55)	(lb/ft^3)	(1.81)	(2.55)
P_c/ℓ_c	202	283	N/m^3	202	283
	(1.28)	(1.80)	(lb/ft^3)	(1.28)	(1.80)
P_c	9269.6	11619.9	N/m^2	13369.1	16758.9
	(193.6)	(242.7)	(lb/ft^2)	(279.2)	(350.0)
ℓ_c	46.0	41.1	m	66.3	59.3
	(150.9)	(134.8)	(ft)	(217.6)	(194.4)
b_c	23.0	20.5	m	33.2	29.6
	(75.5)	(67.4)	(ft)	(108.8)	(97.2)
S	1057.9	843.9	m^2	2200.5	1755.4
	(11387.1)	(9083.7)	(ft^2)	(23685.5)	(18894.6)

TABLE 3 - Sea State Characteristics

Sea State	Avg. Wave Height (meters)	(feet)	Wind Speed (knots)
3	0.88	(2.90)	14.2
4	1.31	(4.4)	17.5
6	2.93	(9.6)	26.2

MODEL DATA SCALING TECHNIQUE

The prediction technique previously discussed is based upon accepted theory and on model and full scale test data. Several empirical equations were discussed that have been derived by scaling model data by a specific method to make them compatible with full scale data. This special model scaling technique has been adopted for scaling the ANVCE model data to make these data compatible with predicted data. The validity of this special technique will be discussed later in this section.

The total drag measured on the model includes hydrodynamic, momentum and aerodynamic drag components. The aerodynamic and hydrodynamic components are scaled differently; therefore, the aerodynamic drag is determined from a series of air tare tests and subtracted from the total measured drag. Air tare tests were conducted with the model suspended above the water and run at various forward speeds. The frontal area created by the basic inflated skirt shape was simulated by a board attached to the bow of the model.

To obtain the total hydrodynamic drag acting on the model, the air tare values or aerodynamic drag and the momentum drag components are subtracted from the measured drag values. This resultant hydrodynamic drag is normally Froude scaled according to the cube of the scale factor, λ^3. However, before this can be computed, these data are "corrected" by the special technique previously mentioned to make these data more representative of full scale conditions.

First, a correction is applied to the calm water model drag data. This correction is intended to account for the scaling of any skirt drag related skirt wetting and the wavemaking effects. These components are difficult to isolate experimentally and to properly scale. In model tests these drag components are grouped into a model residual drag component. Experienced contractors believe that this calm water, residual drag component does not properly scale according to the Froude method. However, if this model drag component is multiplied by a factor of .5 the results obtained by Froude scaling provide a more reasonable

magnitude based upon the limited full scale data that are available. The derivation of this residual scale factor is the result of limited analysis involving sub-scale and full scale data. No documentation of these analyses are available for verification or reference. Application of this scaling factor has resulted in a small reduction in the total scaled calm water drag.

In addition to the correction in calm water, there is a scale factor applied to the drag measured in waves. This scale factor is applied to the scaled wave height instead of the measured drag. Experienced contractors contend that the two-dimensional, long-crested waves generated in tow tank experiments do not simulate the open-ocean, shortcrested waves that a full-scale design would confront in actual operations. Each contractor in the ANVCE Program has selected a given factor for scaling the model wave heights which they believe adequately considers this aspect. For the ANVCE Program, both point design contractors have selected a scale factor of 1.67. A discussion of this factor is presented in Reference 4. This scale factor is based upon an analysis of model and full scale SRN4 data conducted by the British Hovercraft Corporation. Just how representative this factor is for the wave types seen in different oceans as compared to the English Channel, where the SRN4 is operated, is very difficult to address since there is no documentation available on the analysis involved in determining the model wave height scale factor.

To understand how this scaling procedure is used, representative model skirt drag data versus the average wave height for various test speeds are presented in Figure 3. These data are then scaled by the 1.67 factor. For example, the drag measured at an average wave height of .2 feet is plotted at an average wave height of .2 x 1.67 = .334 feet. These scaled drag values are shown by the dashed lines and represent the corrected model skirt drag.

It is now a straight forward procedure to scale the model data to full scale values. The total hydrodynamic model drag (wavemaking

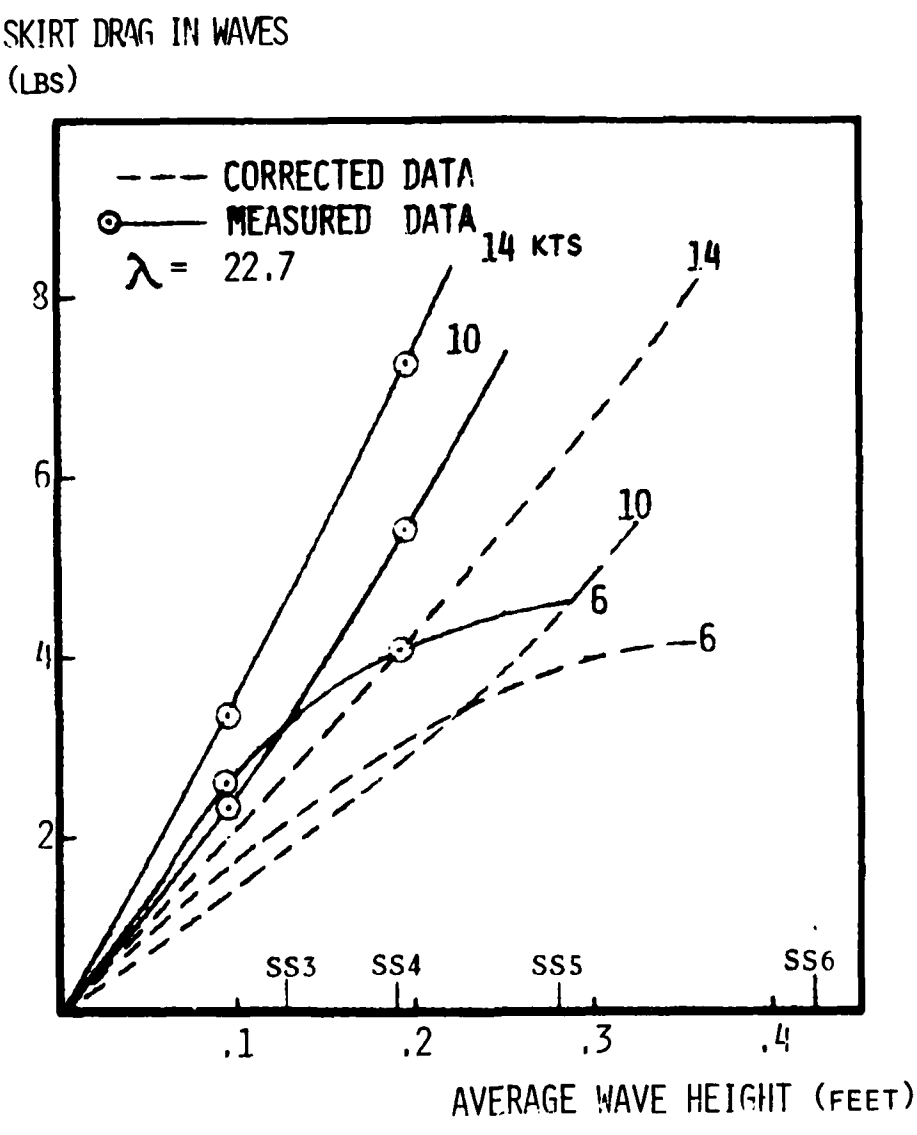

FIGURE 3 - MODEL SKIRT DRAG IN WAVES VERSUS AVERAGE WAVE HEIGHT

and corrected skirt drag) is Froude scaled by the cube of the scale factor, λ^3. The scaled momentum drag is computed from the scaled volume flow rate and the scaled craft velocity in the following equation:

$$D_{MOM} = \rho \cdot Q_{FS} \cdot V_{FS}$$

where ρ = air density

Q_{FS} = full scale volume flow rate

V_{FS} = full scale design velocity

$Q_{FS} = Q_m \cdot \lambda^{5/2}$, where Q_m = model volume flow rate

$V_{FS} = V_m \cdot \lambda^{1/2} + V_{HW}$, where V_m = model velocity

V_{HW} = headwind velocity

λ = scale factor

The aerodynamic drag is based on the full scale design geometry and an aerodynamic drag coefficient equal to .5. The aerodynamic lift coefficient for this analysis is zero. The sum of the hydrodynamic, momentum and aerodynamic drag components is the total full scale design drag. The same momentum and aerodynamic drag components are used in both the presentation of total scaled model results and predicted results. In both presentations of total drag the headwind velocity as a function of sea state (Table 3) is considered in momentum and aerodynamic drag computations.

DISCUSSION OF RESULTS

Representative model drag data in calm water and in random waves have been selected and scaled to the 1000 m ton and 3000 m ton design characteristics for comparison with predicted drag values for these designs. The drag component equations used in this analysis are presented in Appendix A. These equations predict the drag as a function of the design characteristics and operating conditions of speed, sea state, and headwind. The prediction routine can also determine the secondary

hump drag; however, since no attempts were made in the tests to verify these drag values, these analytical results are not presented here.

In Figures 4 through 7,comparisons of the analytically predicted drag and the scaled model drag for the 1000 m ton design are presented for calm water, Sea State 3 and Sea State 4 operation. Predicted and scaled model data for calm water are presented in Figure 4 for two different cushion loadings. The predicted and scaled model data are in very good agreement for the higher full scale cushion loading of $P_c/\sqrt{S} = 400$ N/m^3. These results agree at hump and at moderate speeds; however at high speeds the model results are slightly less than the predicted results. At the lower cushion loading, $P_c/\sqrt{S} = 285$ N/m^3, the scaled model drag is from 4-percent at hump speed to 27-percent at 90 knots lower than the predicted drag. The flow rate for this case is twice that tested at the higher cushion loading providing a gap height of .15 meters (.5 ft) compared to .075 meters (.25 ft).

Factors that may contribute to possible drag discrepancies are insufficient volume flow rate or non-optimum pitch trim of the model during free to heave and free to pitch experiments. Average model trim angle, heave position and total drag versus model velocity are presented in Figure 5 for the calm water tests. At the higher cushion loading, $P_c/\sqrt{S} = 400$ N/m^3, two model flow rate conditions of $Q_m = 0.76$ cms (8.2 cfs) and 1.1 cms (11.8 cfs) were tested. These results show a substantial reduction in the drag for a nominal increase in the flow rate. The model trim data are very similar; however, at the lower flow rate condition the model heave position is also the lowest and decreases at higher speed,which appears to result in higher drag. There are insufficient data to formulate any conclusions as to what is the optimum flow rate; however, it is believed that these results do indicate that the model at the higher flow rate had near-optimum flow rate with satisfactory trim and heave characteristics.

In contrast to the test results previously discussed, additional tests were conducted that represented a scaled 1000 m ton configuration

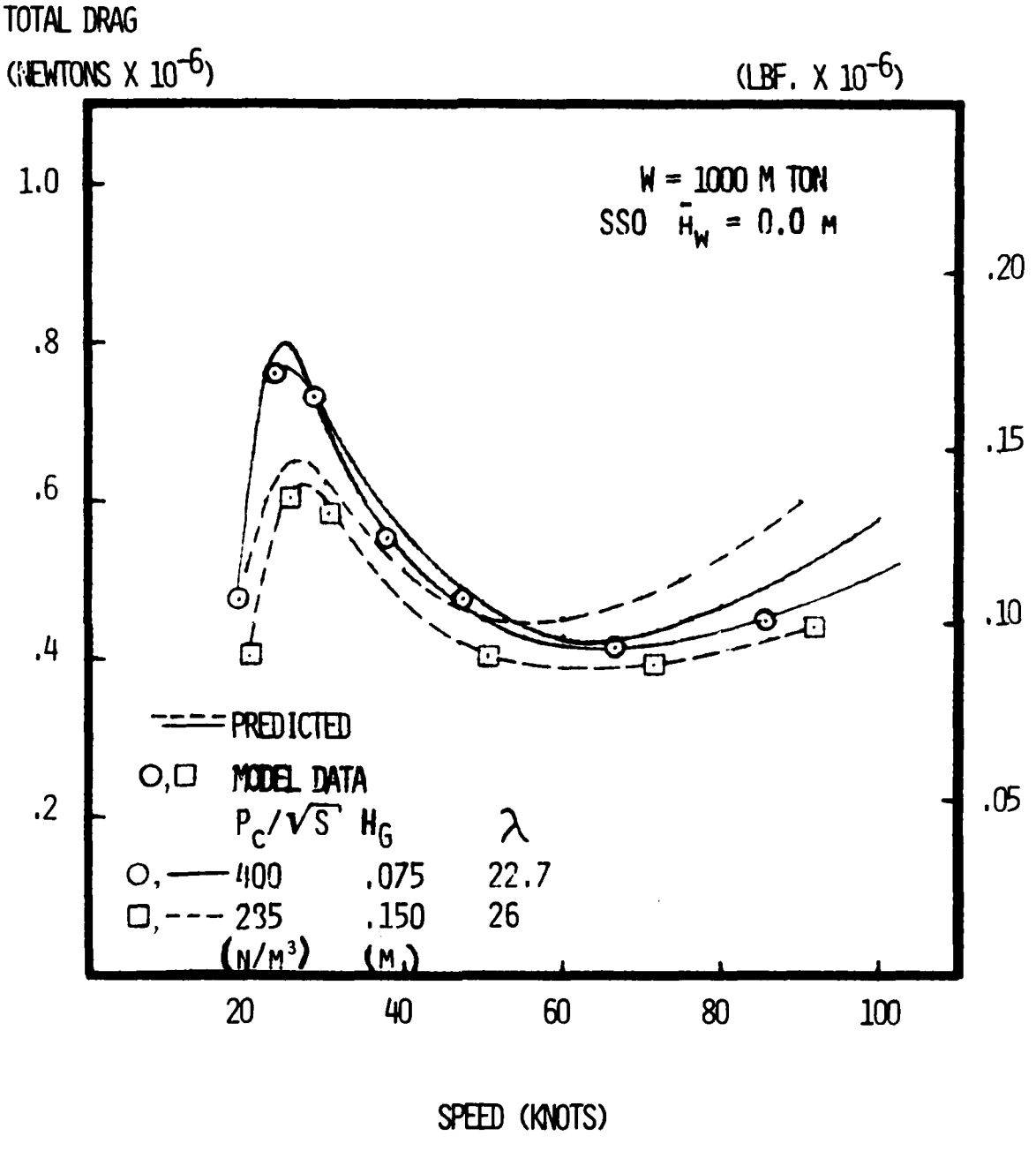

FIGURE 4 - COMPARISON OF MODEL AND PREDICTED TOTAL DRAG VERSUS SPEED FOR THE 1000 M TON ACV IN CALM WATER

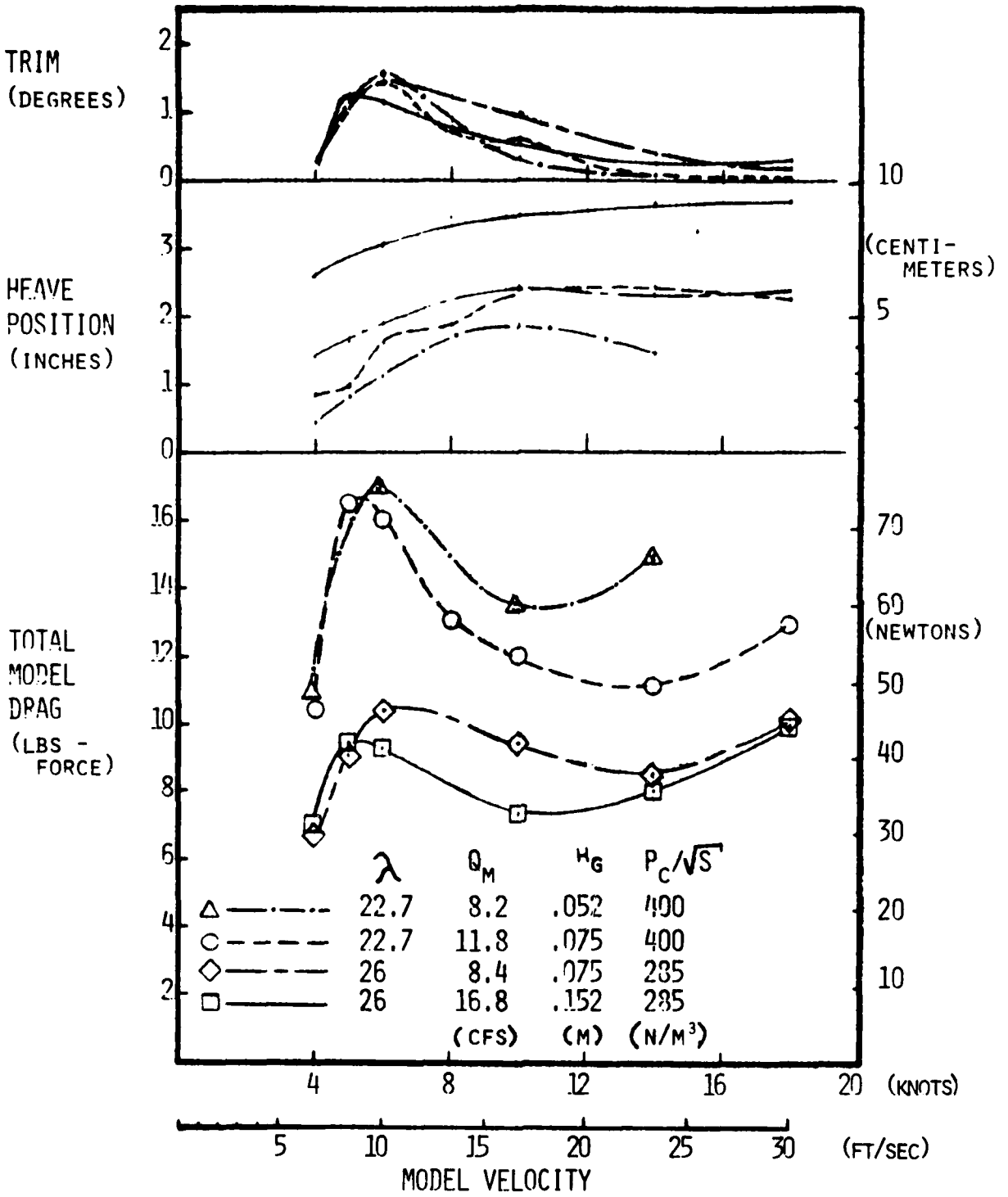

FIGURE 5 - REPRESENTATIVE MODEL TEST DATA VERSUS VELOCITY

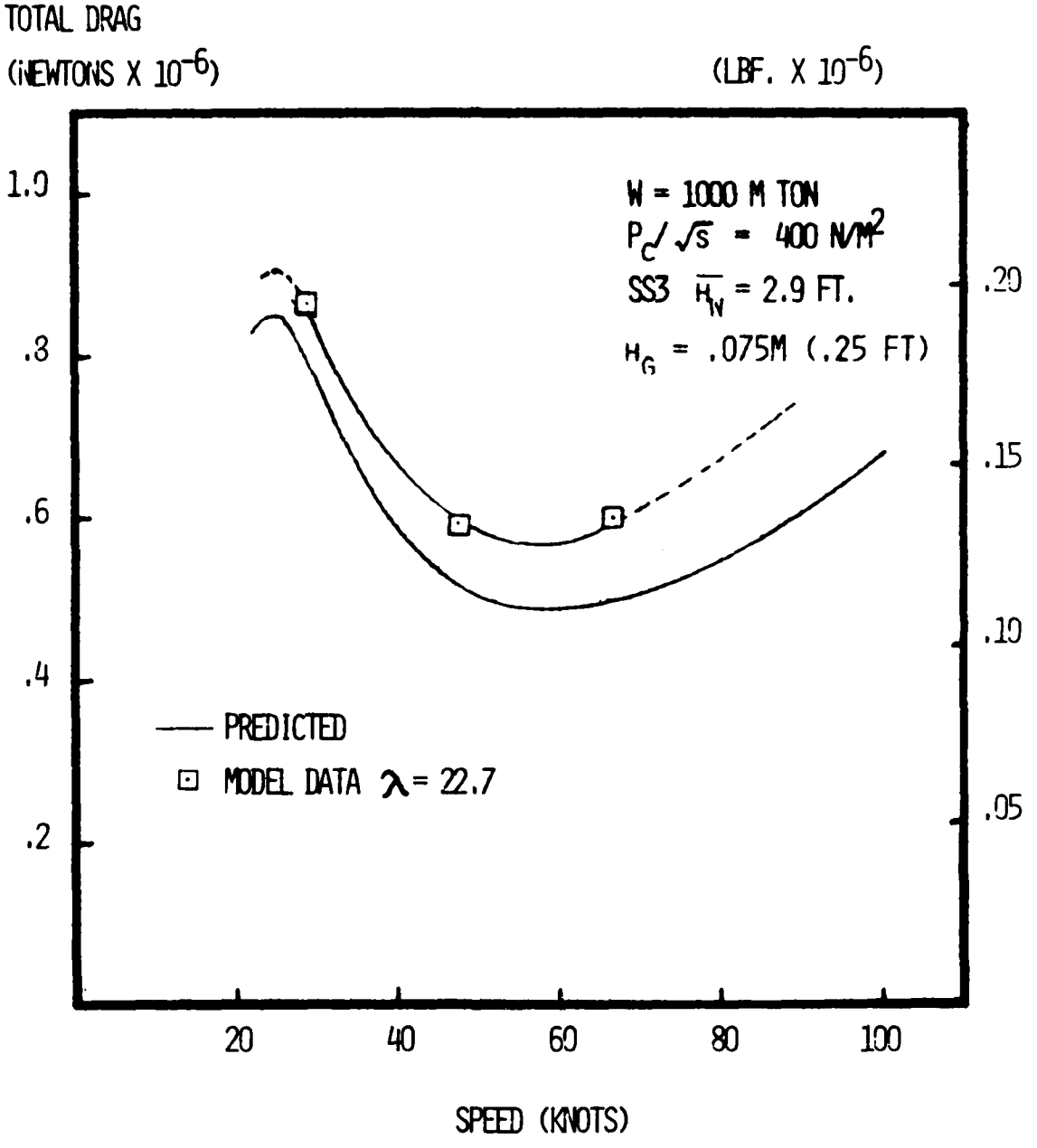

FIGURE 6 - COMPARISON OF MODEL AND PREDICTED TOTAL DRAG VERSUS SPEED FOR THE 1000 M TON ACV IN SEA STATE 3

at a full scale cushion loading of $P_c/\sqrt{S}$ = 285 N/m^3. In Figure 5, the total model drag for this condition is less than the drag at $P_c/\sqrt{S}$ = 400 N/m^3 due to the lower wave making drag component. At the lower cushion loading, the results indicate a different trend from those previously discussed. By doubling the model flow rate from .78 cms (8.4 cfs) to 1.56 cms (16.8 cfs), the model drag has decreased only at the intermediate model velocities of 6 and 10 knots. Very little decrease resulted at the higher velocities where the most substantial drag decrease occurred for the higher cushion loading tests. The model data indicate a uniform difference in heave position for the two flow rate conditions; however, the trim data indicate a somewhat larger difference at the intermediate velocities when compared to the previous data at $P_c/\sqrt{S}$ = 400 N/m^3. The double amplitude pitch results, which are not presented, are substantially greater at 6 and 10 knots for the Q_m = .78 cms condition when compared to these data at other velocities. This deviation at only these speeds is difficult to explain for calm water tests. Since the model did pitch excessively for calm water operation, it does appear that the test data at 6 and 10 knots are questionable.

Predicted and scaled model total drag results for operation in waves are presented in Figures 6 and 7. For these tests, data at the higher cushion loading of $P_c/\sqrt{S}$ = 400 N/m^3 were selected. Comparisons of these data for Sea States 3 and 4 indicate that greater model drag were measured than analytically predicted for the same conditions. In Figure 6, the scaled model drag for Sea State 3 is shown to be from 8 to 20-percent greater than the predicted drag depending upon the speed. The scaled model drag is from 10 to 25-percent greater in Sea State 4 than the predicted drag distribution. See Figure 7. From these scaled model results it appears that the drag degradation due to waves is not only larger than that computed by predictive technique, but the difference is greater with increasing wave height. Results for Sea State 6 were not computed since an unreasonable extrapolation of the model data would have been necessary.

To obtain data for larger gross weight conditions, tests were also conducted for a scaled 3000 m ton configuration at several cushion loadings.

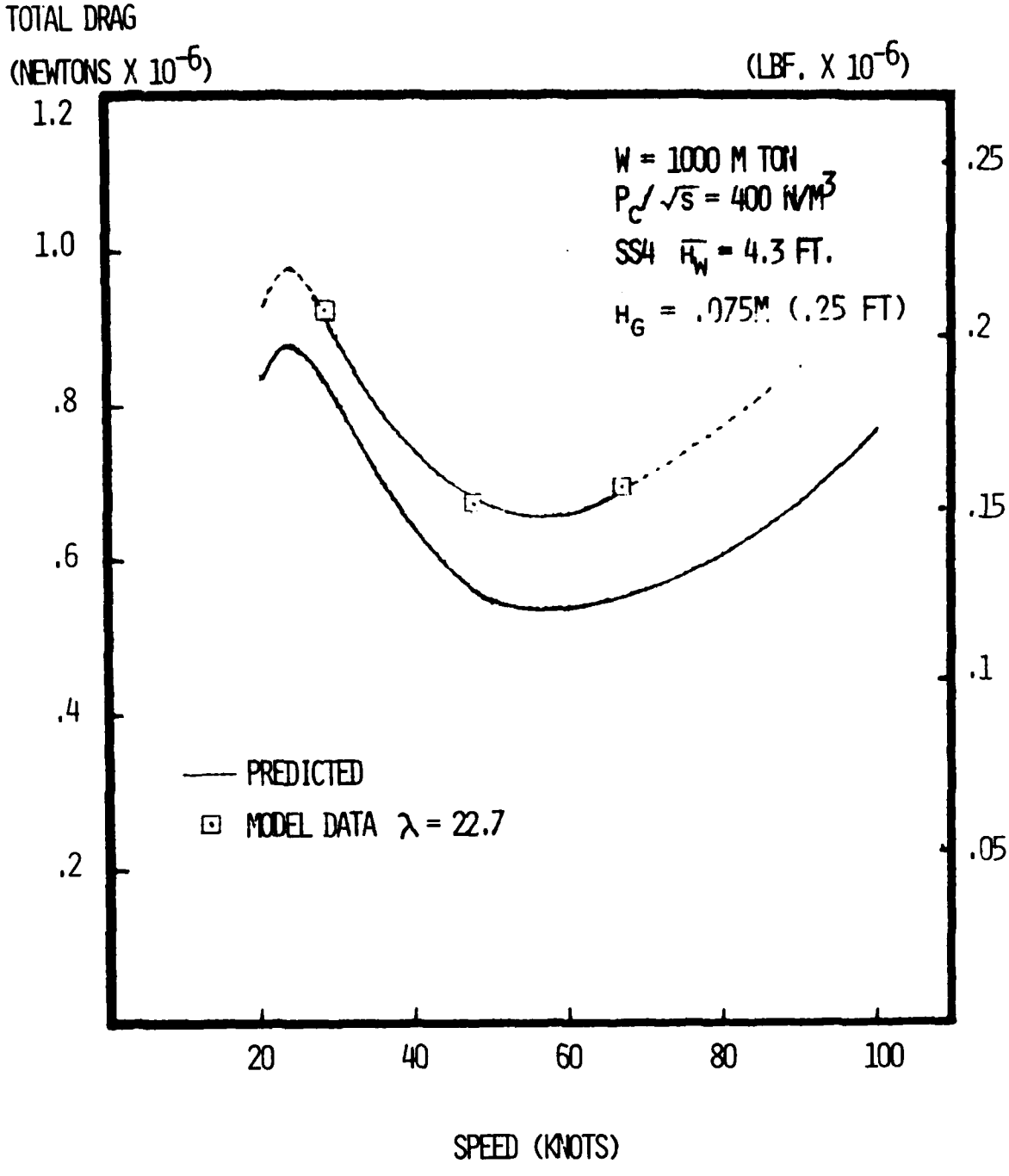

FIGURE 7 - COMPARISON OF MODEL AND PREDICTED TOTAL DRAG VERSUS SPEED FOR THE 1000 M TON ACV IN SEA STATE 4

This required that a large scale factor of $\lambda = 37.5$ be used for proper scaling of the model data. Results at a cushion loading of 285 N/m^3 have been selected for presentation. Initial calm water tests were conducted at several different model flow rate conditions (Reference 2). In Figure 8, the scaled model drag for these tests are presented for equivalent full scale gap heights of .11, .15 and .22 meters. Predicted drag results are also presented for gap heights of .11 and .22 meters. These data indicate that the analytical technique does not predict any substantial changes in the various drag components due to increases in the flow rate. For the increase in flow rate or equivalent gap height shown, the momentum drag doubles and the calm water skirt wetting drag component decreases slightly. The net effect on the full scale total drag is very small.

The model results presented in Figure 8 do not totally agree with the insensitivity of the predicted drag due to changes in gap height. At the low and high speeds tested, very little differences in the drags exist; however, at the intermediate speeds of 37 and 61 knots there is a confusing deviation in the drag. These results are the model data presented in Figure 5 that have been scaled by the appropriate scale factor. It was previously discussed that without sufficient repeat data points, it is difficult to substantiate whether or not these data are accurate. From the data available, it is impossible to explain why the drag is higher at only these speeds and why the drag at $Q_m = 1.1$ cms ($h_g = .15$ m) is higher than the drag at the lower model flow rate of $Q_m = .76$ cms ($hg = .11$ m) with consideration for the difference between the momentum drag components.

In order to proceed with the analysis of the rough water drag, it was necessary to determine the total calm water drag at the flow rate used for the rough water tests. This flow rate provides a full scale equivalent gap height of .12 meters. From the analysis of the model test results, the scale model total calm water drag for this condition was determined to be the drag presented in Figure 9. The data symbols shown indicate that these are points based upon actual test data; however, no data were actually measured for this flow rate condition.

The calm water drag presented in Figure 9 at a speed of 61 knots is slightly lower than what would be determined from a straight forward interpolation of the drag data presented in Figure 8. This variation in the drag is justified based upon previous test data and the general agreement of the drag results at higher and lower speeds. It should also be noted that the scaled model drag is less than the predicted calm water drag at high speeds which is similar to the data presented for the 1000 m ton case.

Also presented in Figure 9 are the total scaled model and predicted drag in Sea State 3. The scaled model results are shown to be in good agreement with the predicted drag for this sea state condition. It also should be noted that the scaled model results are slightly lower than the predicted drag at hump speed. This is some indication that the model is operating at very near the optimum trim condition.

Although the results in Sea State 3 are in favorable agreement, model results for the 3000 m ton design in higher sea states follow the trend of the previous 1000 m ton data. In Figure 10, scaled model data and predicted drag results show good agreement near hump speed; however at higher speeds, such as 85 knots, the scaled model drag is shown to be 16-percent greater than the predicted drag. Better agreement was anticipated at the lower cushion loading; however, this discrepancy is an improvement compared to the 1000 m ton results at the higher cushion loading. For Sea State 6, the comparison of the results indicate that the scaled model drag is also substantially greater than the predicted drag. These drag results are presented in Figure 11 and show that the scaled model drag to be 28-percent greater than the predicted results at a speed of 61 knots.

It is difficult to explain the possible reasons for the poor correlation of the scaled model and analytical results in waves. The obvious contributor to the discrepancy is the rough water skirt drag component. The scaling procedures used have reduced this skirt drag or residual drag component somewhat; however, the scaled skirt drag component is still substantially greater than that predicted. This

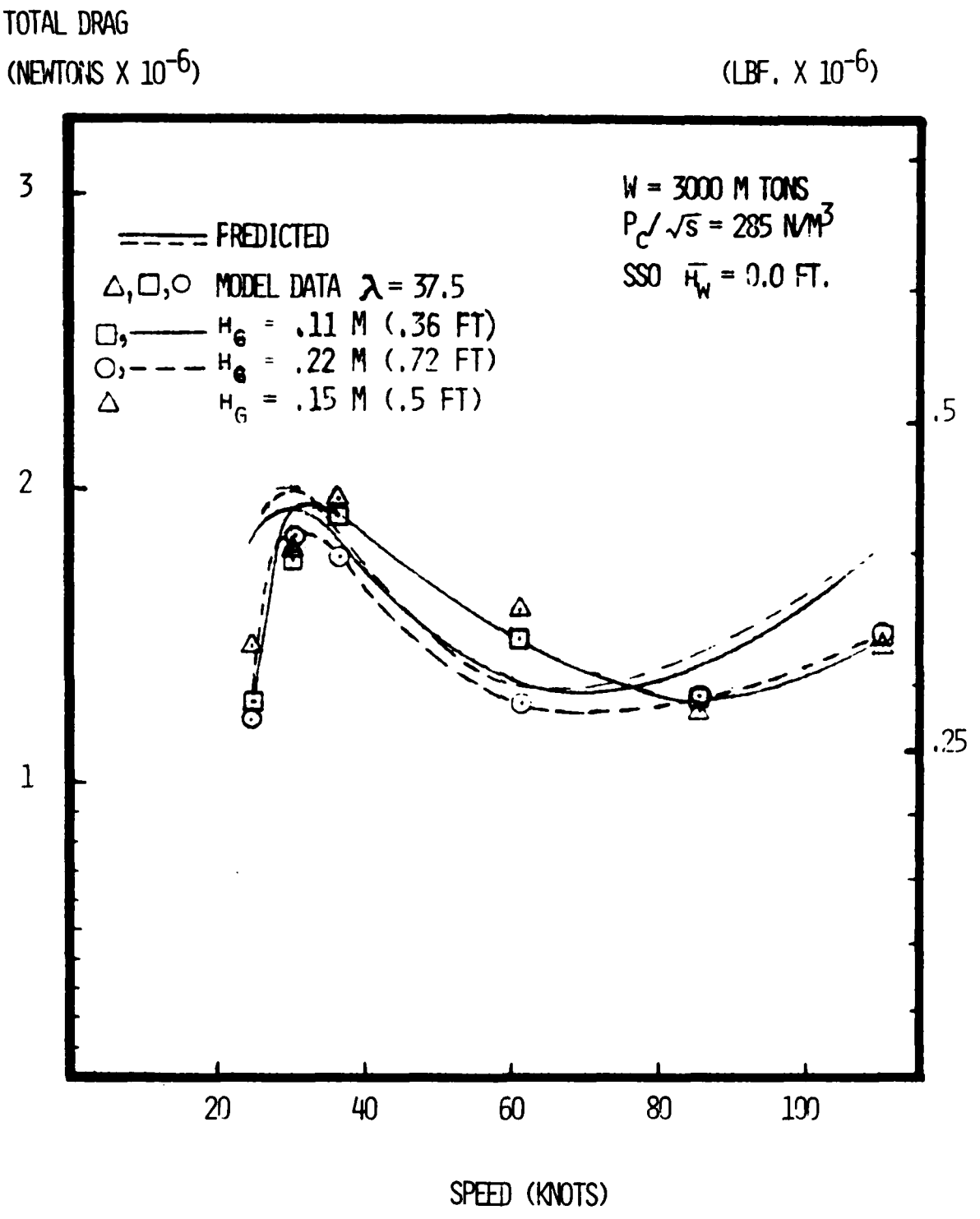

FIGURE 8 - COMPARISON OF MODEL AND PREDICTED TOTAL DRAG VERSUS SPEED FOR THE 3000 M TON ACV IN CALM WATER

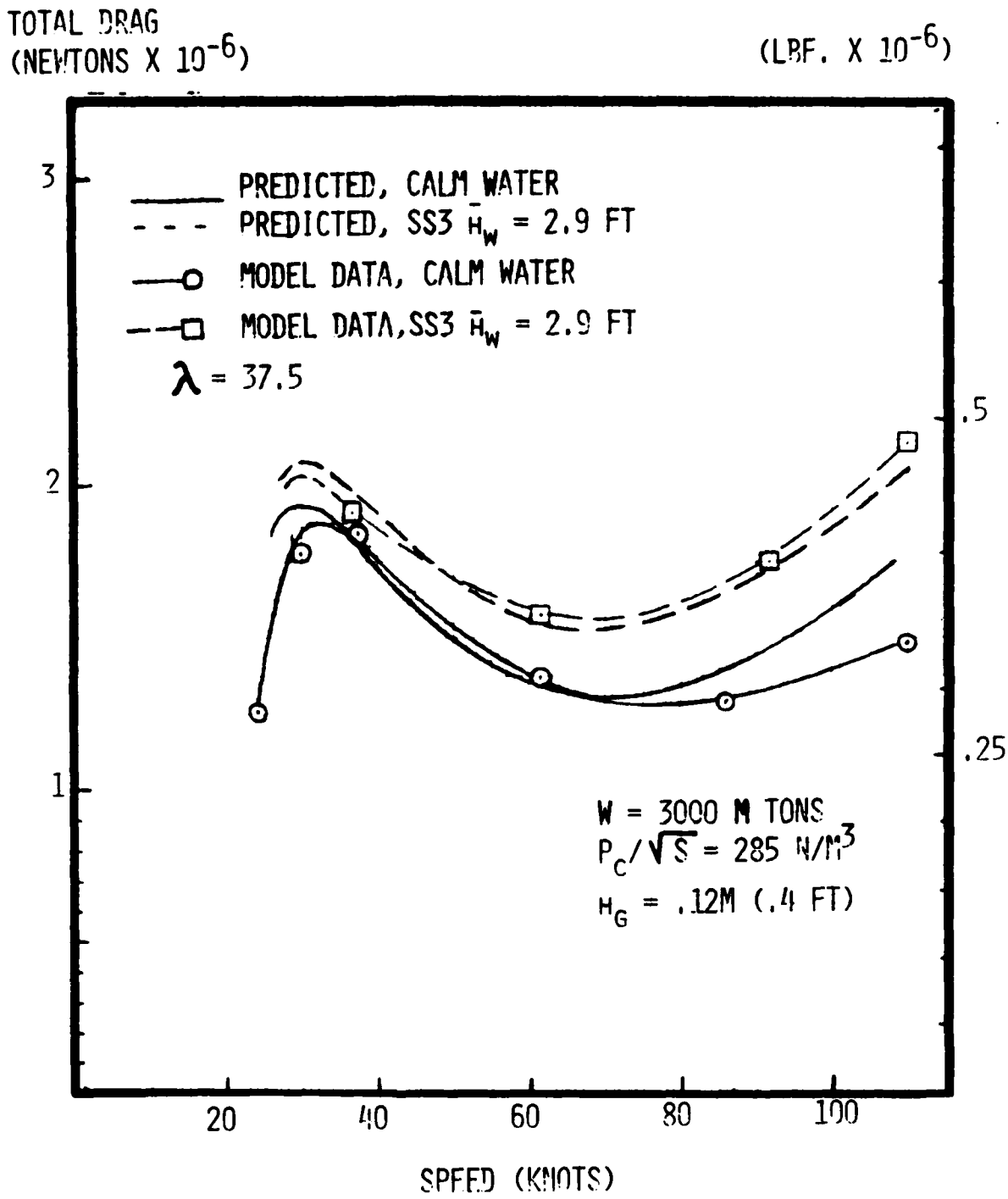

FIGURE 9 - COMPARISON OF MODEL AND PREDICTED TOTAL DRAG VERSUS SPEED FOR THE 3000 M TON ACV IN CALM WATER AND SEA STATE 3

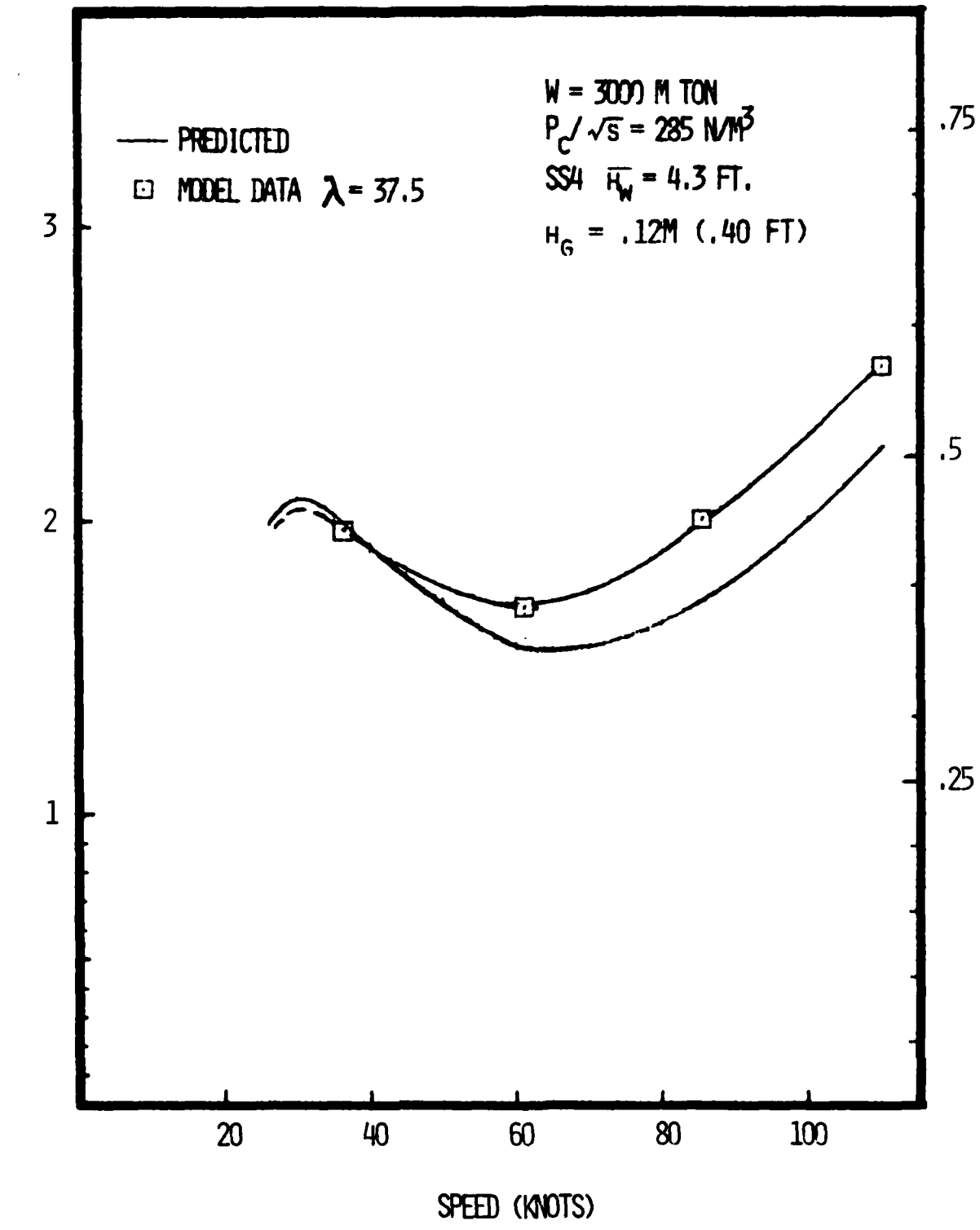

FIGURE 10 - COMPARISON OF MODEL AND PREDICTED TOTAL DRAG VERSUS SPEED FOR THE 3000 M TON ACV IN SEA STATE 4

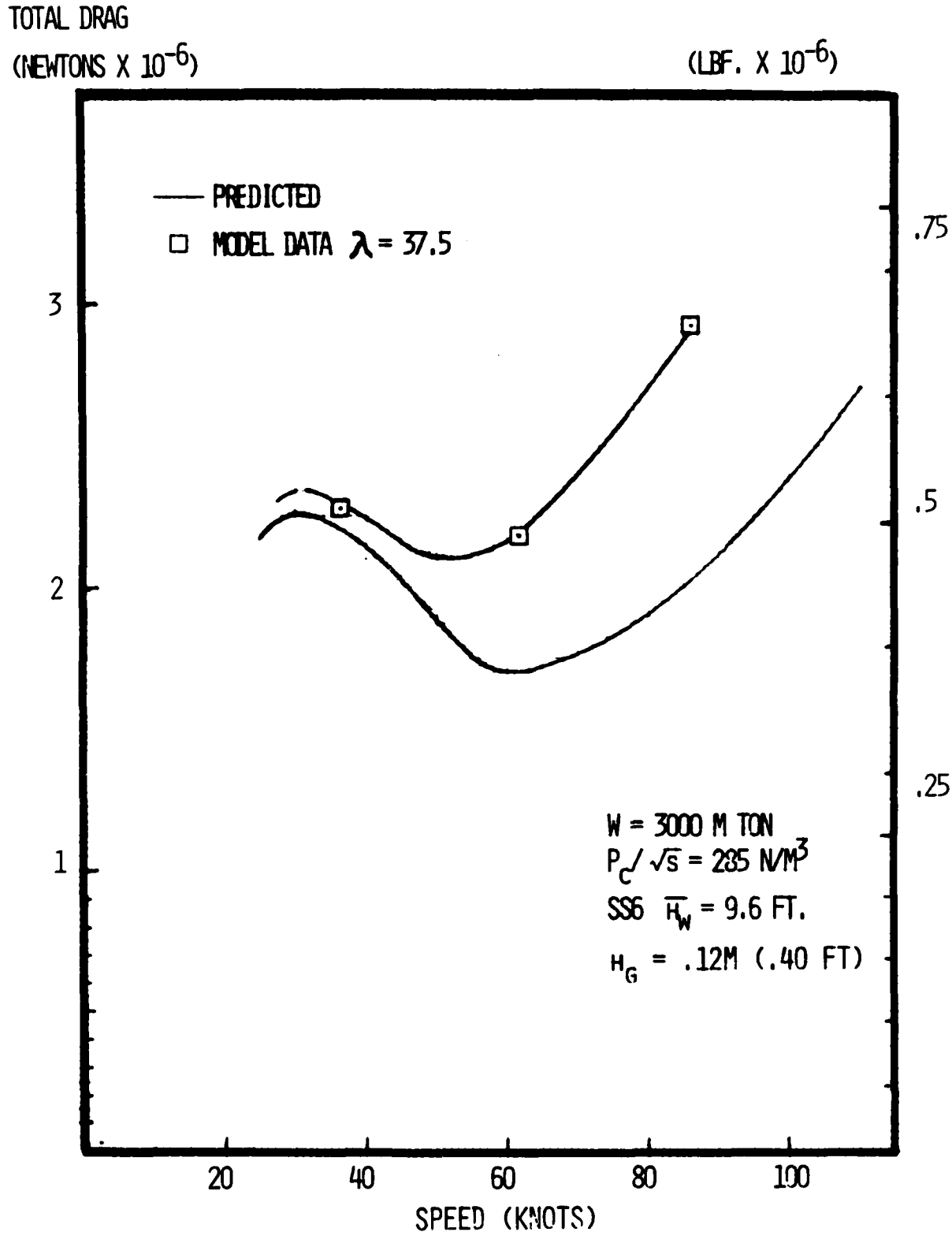

FIGURE 11 - COMPARISON OF MODEL AND PREDICTED TOTAL DRAG VERSUS SPEED FOR THE 3000 M TON ACV IN SEA STATE 6

is evident from the data presented in Figure 12. The rough water skirt drag is presented versus wave height for different velocities. The corrected drag is shown to be approximately 2 to 2.5 times greater than the predicted drag. The predicted and corrected scaled data appear to be proportional to the wave height and vary according to the velocity squared.

The empirical relationships used in the analytical predictions were derived from model and full scale data measured at significantly lower cushion loadings and gross weights. All the data used were based on bag/finger skirt configurations that provide a relatively low cushion depth. The bag/finger skirt system also utilized longitudinal and lateral stability seals that compartment the cushion and contribute to the total skirt drag. The loop-pericell skirt configuration selected for these tests represents a deep cushion skirt design and does not require any stability seals.

The analytical skirt drag equation for rough water is presented in Appendix A, Figure A-2. The rough water drag equation presented is based on bag/finger skirt designs with a finger height, h_f, and a cushion height, h_c. For this analysis, the pericell height is considered equivalent to the finger height, and there is no difference in the cushion height term between the bag/finger and the loop pericell skirt designs. Since only limited model test data are available on loop-pericell skirt designs, no attempts were made to address the stiffness of an individual pericell as compared to an individual finger of identical height. This can obviously make a difference in the skirt response due to wave impacts and the associated vehicle motions and skirt drag.

All the discrepancies between the model and predicted data cannot be attributed to possible inadequacies in the prediction technique. Certain model and testing aspects may have been responsible. It is not known whether or not the problems with the skirt attachment may have contributed to an increase in drag. Previous tests have indicated that the pericell skirt has minimum drag at a trim angle of approximately 1 degree

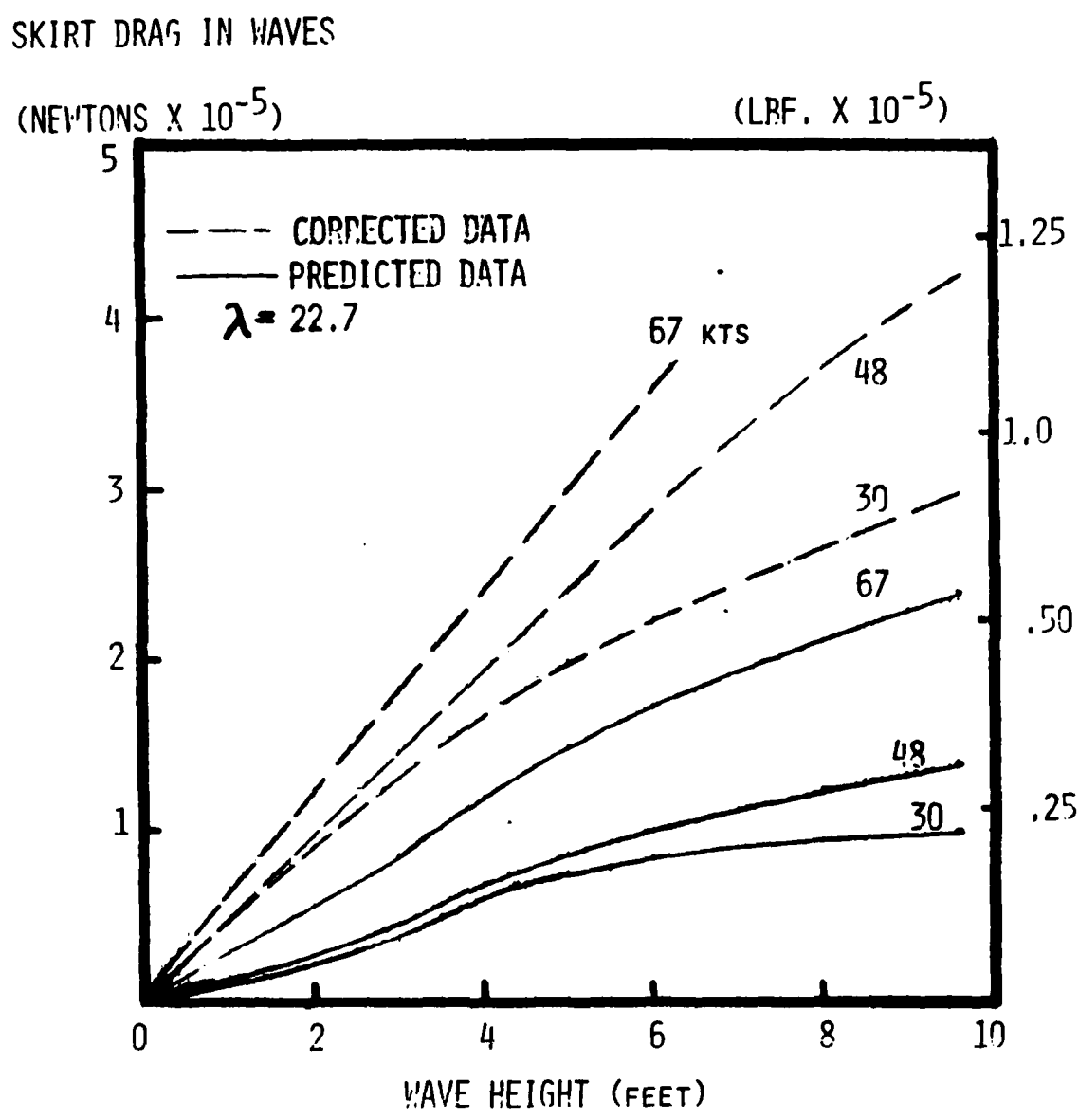

FIGURE 12 - SKIRT DRAG IN WAVES VERSUS WAVE HEIGHT AS A FUNCTION OF VELOCITY

or less. Due to time constraints of the test, only limited runs were made to optimize the trim angle; however, test results, such as those presented in Figure 4, show that the trim angle was within this range at speeds other than hump speed.

The limited tests also did not allow for the optimum flow rate for each design case to be determined. Normally a complete test series of various flow rates would have to be conducted to identify the flow rate at which minimum drag occurred. Results presented in this report have shown that the higher model flow rates tested have the lowest total model drag. The fact that the tests were not conducted at optimum flow rate may have contributed to some of the increased drag. However, sufficient data were not fathered to determine if the difference between the present total drag and the unknown total drag measured at the optimum flow rate would be substantial. From the data gathered it is doubtful that substantial drag reductions, by increasing or reducing the flow rate, can be achieved.

CONCLUSIONS AND RECOMMENDATIONS

The drag comparisons of the scaled model and the predicted drag presented herein have shown reasonable agreement for calm water and some substantial differences for rough water depending upon design weight, cushion loading and speed. From the results presented, it appears that the prediction technique is adequate for assessing the performance of ACV designs operating in calm water and up to Sea State 3. Results compiled for designs with high cushion loadings operating in Sea State 3 should be considered slightly optimistic due to drag differences that were presented in Figure 6. From the results presented herein, it would be unadvisable for the present prediction technique to be used for determining ACV performance in sea states higher than Sea State 3. This would apply to ACV configurations employing a loop-pericell skirt system.

From an evaluation of the other test results, it is believed that a deep loop-pericell skirt can be designed to operate with less sea state drag degradation. There is no new information to indicate that the present technique cannot adequately predict the rough water skirt drag for a bag/finger skirt system in all sea states. It is very possible that the drag degradation for the bag/finger skirt system in higher sea states should be somewhat greater for designs with high cushion loadings than the drag degradation presently predicted, however; there are no test data to substantiate this assertion.

It is apparent that the present technique does not adequately predict changes in drag as a function of the flow rate condition. This is a significant aspect, since determination of the optimum flow rate can influence the motion and ride characteristics, the drag characteristics, and the lift system design characteristics. In Reference 6, the contractor has included new analyses which attempts to predict the change in skirt drag due to variations in flow rate. This analysis was not received in time to be considered in the evaluation of data presented in this report; however, this analysis does indicate that the flow rates selected for the ANVCE tests were reasonably close to the optimum flow rates as defined in the analysis.

It is highly recommended that additional tests should be conducted upon specific skirt configurations at different cushion loadings, cushion flow rates, model weights and sea states to provide an increased data base. These data could then be utilized to improve the capability of the prediction technique particularly in higher sea states and allow for the assessment of the performance degradation at off-design or non-optimum conditions.

It is also recommended that the ANVCE Program Office request that further updating of the prediction technique be considered based upon information and data furnished in the final point design reports. This updating will allow the ANVCE Program Office to conduct an independent assessment of the performance capability of each point design. An evaluation of the performance techniques used by each contractor will also enable the ANVCE program to substantiate the performance capability claimed by each contractor for their point designs.

APPENDIX A

The drag of an ACV consists of four components. The four components are:

(1) Aerodynamic drag

(2) Momentum drag

(3) Wavemaking drag

(4) Skirt drag

(1) The aerodynamic drag is the component of drag caused by skin friction and form drag on the ACV. The equation is:

$$D_A = C_D \cdot q \cdot (h/b) \cdot b^2$$

where q is the dynamic pressure (lb/ft^2), b is the beam (ft), and h/b is the overall height to beam ratio.

The product of h/b x b^2 is a computation to find the frontal area of the craft (assuming a rectangular area). C_D is the drag coefficient based on frontal area. From wind tunnel tests of various ACVs, it has been found that 0.5 is a good approximate value for C_D.

(2) The momentum drag or ram drag results when a constant mass flow rate of air is changed from a velocity relative to the ACV to a zero velocity relative to the ACV. Thus,

$$D_M = V \cdot \rho_a \cdot Q$$

where V is the velocity of the craft (ft/sec), ρ_a is the mass density of air at 15 degrees C (lb/ft^3), and Q is the volume flow rate (ft^3/sec).

(3) An ACV generates a wave after the pressurized plenum passes over a body of calm water. This is of interest, because the pressure region ultimately acts on the vehicle to give a resultant air pressure force tilting back from the vertical. This tilted force, in addition to a lift component, has a drag component which is called wavemaking drag, D_W.

Newman and Poole have done extensive work in this area for a rectangular distribution of constant pressure. Their equation for the wavemaking drag to lift ratio (or drag/weight ratio) is,

$$\frac{D_W}{L} = \frac{4P_c}{\rho_w g \ell} \cdot f_\ell \qquad \text{(Ref. 4)}$$

where L is the lift in pounds, ρ_w is the mass density of water (lb/ft^3), g is the acceleration of gravity (ft/sec^2), P_c is the cushion pressure (lb/ft^2) and ℓ is the cushion length (ft). From Newman and Poole's work, the value of the wave drag parameter, f_ℓ, was shown to be a function of length to beam ratio, ℓ/b and the Froude number, $F_\ell = V/\sqrt{g\ell}$ (where V is the velocity in ft/sec). The variations of the wave drag parameter versus Froude number for various length to beam ratios are presented in Figure A-1. These data have been compiled in the parametric design analysis computer program to determine the wavemaking drag as a function of Froude number and design length to beam ratio.

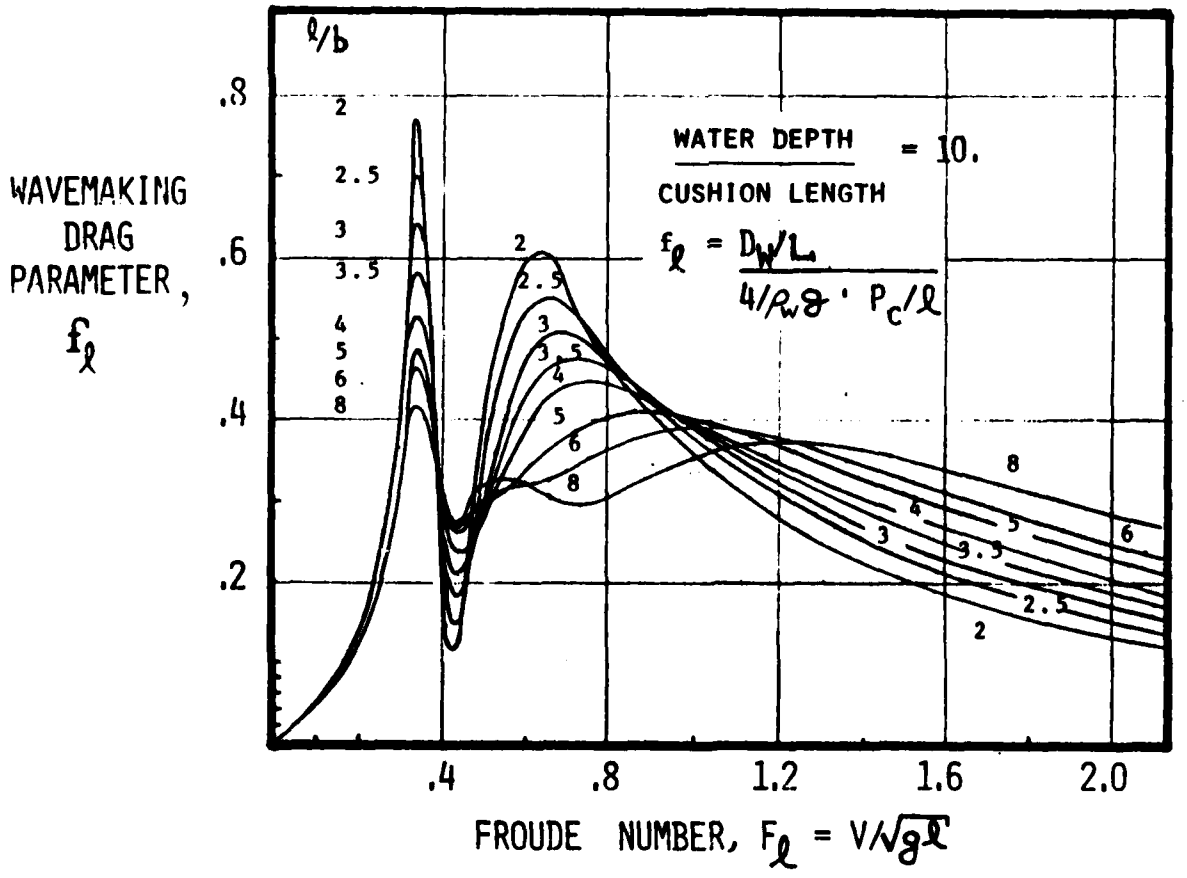

Figure A-1 - Wavemaking Drag Parameter versus Froude Number as a Function of Length to Beam Ratio

(4) There are limited techniques available for determining the skirt drag component. One technique was selected as having the most representative trends with the dependent variables. In this technique, the skirt drag component has three parts. A calm water wetting drag term, DSKCW, is characterized by the following empirical equation,

$$DSKCW = 9.82 \cdot 10^{-6} \cdot (h_g/P)^{-.34} \cdot P \cdot S^{1/2} \cdot V_k^2 \qquad \text{(Ref. 3)}$$

where h_g is the gap height (ft), P is the skirt perimeter (ft), S is the cushion area (ft^2) and V_k is the velocity in knots. The second item is the skirt wave making drag, DSKWM, which is based on the D_W calculated previously. This component is determined by the following expression:

$$DSKWM = D_W \cdot \left[\frac{1.50}{P_C/\sqrt{S}^{.2588}} - 1 \right]$$

where $P_C/\sqrt{S}$ is the cushion pressure divided by the square root of the cushion area (lb/ft^3).

The last component of skirt drag is the rough water component, DSKRW. This component has been derived from model and full scale skirt drag data which have been determined as a function of skirt geometry and wave height (Reference 3). These data are shown in Figure 2-A where YSK is the rough water skirt drag parameter and XSK is a function of the wave height, cushion height and skirt finger height which is usually 40 to 60 percent of the cushion height for bag finger skirt designs.

The rough water skirt drag is computed from the following empirical expression:

$$DSKRW = 2.84 \cdot 10^{-5} \cdot YSK \cdot 1/2\, \rho_w V_K^2 \cdot P \cdot \sqrt{S} \cdot DSKRWFC$$

where YSK is determined from curve fit of data shown above and,

$$DSKRWFC = 1 + \tan \left[\left(\pi/3.5449 \cdot \left(1 - \frac{|V_K - V_H|}{V_H}\right) \right)^2 \right]$$

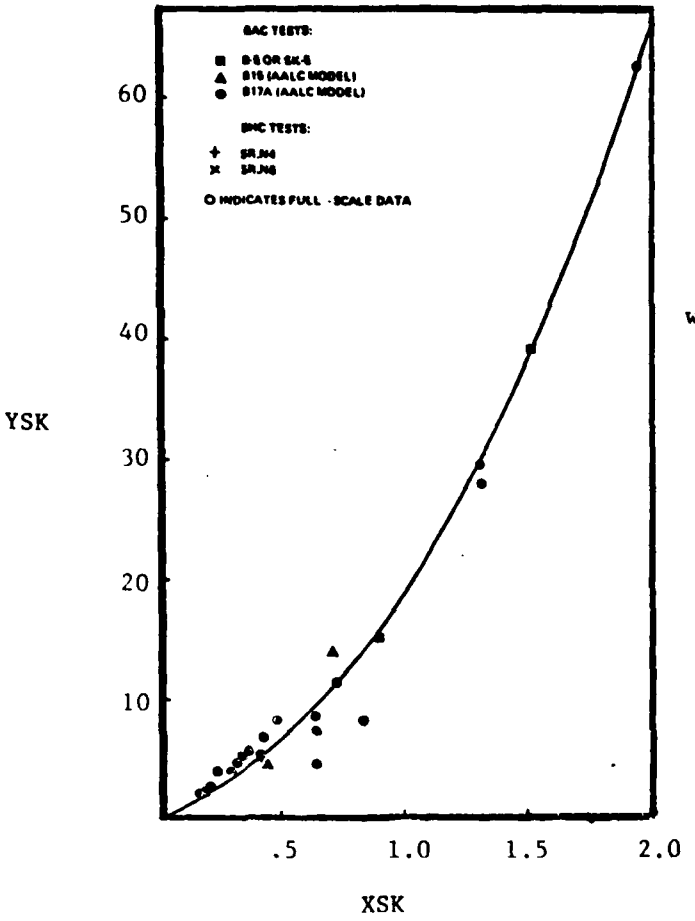

CURVE FIT: $YSK = f(XSK)$

$$YSK = A \cdot XSK^3 + B \cdot XSK^2 + C \cdot XSK + D$$

where

$$XSK = \frac{2\, h_w}{h_c + h_f}$$

$A = 1.517$

$B = 9.476$

$C = 7.754$

$D = .107$

h_w = average wave height (ft)

h_c = cushion height (ft)

h_f = finger height (ft)

Figure A-2 - Skirt Drag Prediction in Waves

The rough water skirt drag friction coefficient, DSKRWFC applies for velocities $V_{HUMP} \leq V_K \leq 2\, V_{HUMP}$ to account for increased seal wetting due to craft motion near hump. The units of the other terms in the equation are:

ρ_w = density of water (lb/ft^3)

V_K = velocity (knots)

P = skirt perimeter (ft)

S = cushion area (ft^2)

V_H = hump velocity (knots)

It should be emphasized that these skirt drag equations are empirical equations that are based upon limited scale model and full scale ACV experimental drag data. This rough water data has been compiled from two dimensional scaled waves and estimates of open ocean wave heights. Data on the sea spectrum used, Pierson-Moskowitz or others, and the energy

levels in each sea state are not available. Scaling factors have also been applied to the model data which have not been completely verified. The drag data used are based upon low cushion pressure and conventional skirt height designs; however, the equations do consider those critical parameters which describe the advanced ACV concepts considered in this report.

REFERENCES

1. Graff, R. O., LeBeau, R. P., "A Parametric Study of Air Cushion Vehicles Prepared for the Advanced Naval Vehicle Concept Evaluation Study," David W. Taylor Naval Ship Research and Development Center, Aviation and Surface Effects Dept., TM 16-77-98 (Sep 1976).

2. Gersten, A., "Motions and Drag of a Air Cushion Vehicle with Deep Skirts in Calm Water and Random Waves," David W. Taylor Naval Ship Research and Development Center, Ship Performance Dept., SPD-748-01 (Jan 1977)

3. "Arctic Surface Effect Vehicle Program," Bell Aerospace Corporation, ARPA Order No. 1967, Volume I Task 2.1.1 (Feb 1973).

4. Chaplin, H. R. and Ford, A. G., "Some Design Principles of Ground Effect Machines, Section D-Drag," DTMB Report 2121D (Jun 1966).

5. "Arctic Surface Effect Vehicle Program - Configuration Studies Technical Progress Report Volumn 2 - Model Test Program," Aerojet-General Corporation, Report No. (AGC-T-462) (Jan 1974).

6. "Advanced Naval Vehicles Concepts Evaluation Point Design for 3000-Ton Cushion Vehicle (U)," Bell Aerospace Corporation, Report 7588-950049 (Jan 1977) Confidential.

DTNSRDC ISSUES THREE TYPES OF REPORTS

(1) DTNSRDC REPORTS, A FORMAL SERIES PUBLISHING INFORMATION OF PERMANENT TECHNICAL VALUE, DESIGNATED BY A SERIAL REPORT NUMBER.

(2) DEPARTMENTAL REPORTS, A SEMIFORMAL SERIES, RECORDING INFORMATION OF A PRELIMINARY OR TEMPORARY NATURE, OR OF LIMITED INTEREST OR SIGNIFICANCE, CARRYING A DEPARTMENTAL ALPHANUMERIC IDENTIFICATION.

(3) TECHNICAL MEMORANDA, AN INFORMAL SERIES, USUALLY INTERNAL WORKING PAPERS OR DIRECT REPORTS TO SPONSORS, NUMBERED AS TM SERIES REPORTS; NOT FOR GENERAL DISTRIBUTION.